

GEOPHYSICAL SURVEYS AT PORT CARLISLE, CUMBRIA 2021

REPORT BY ALEX TURNER



Extract from Christopher Saxton's map of England and Wales, 1579

Table of Contents

Table of Contents	1
Table of Figures	2
Introduction.....	3
Location	3
Topography and Geology	5
Topography.....	5
Geology.....	5
Survey Methodology	7
Methods - Survey Grids and Markers.....	7
Methods - Fluxgate gradiometer survey	8
Methods – Electrical resistance survey	8
Data processing and presentation.....	9
Reference to Historic Ordnance Survey	9
Survey Results and Interpretation.....	10
Gradiometer Results – process summary.....	10
Gradiometer Results – Interpretation	12
Resistivity Results – process summary	12
Resistivity Results – Interpretation	12
Summary.....	14
Sources and References	14

Table of Figures

Figure 1 - Location of Port Carlisle. The area of interest is within the red rectangle	3
Figure 2 - MC79 excavation 1999 (Wilmott 2012, 193) in relation to geophysics from 2020 and 2021	4
Figure 3 - Flood risk from the sea in relation to the site location.....	4
Figure 4 - Lidar digital terrain model (DTM) of the survey areas. The raised line of the wall is clearly visible within the bounds of the World Heritage Site boundary (shown in black).....	5
Figure 5 - Bedrock geology for the survey area. BGS 1:50,000 digital geology data.	6
Figure 6 – Superficial geology for the survey area. BGS 1:50,000 digital geology data.....	6
Figure 7 – Soil data (Parent material) for the survey area. BGS 1:50,000 digital geology data.....	7
Figure 8 - Location and numbering of the gradiometer survey grids.	8
Figure 9 - Field boundary layout shown on the Ordnance Survey 1:2500 County Series 1895.....	9
Figure 10 - 1:2500 Ordnance Survey map (1970) showing location of a small building on the field boundary.....	10
Figure 11 - Plot of the gradiometer survey results	11
Figure 12 - Interpretation of the gradiometer survey results.....	11
Figure 13 - Plot of results from the resistivity survey	12
Figure 14 - Interpretation of the resistivity survey results	13
Figure 15 - 3D view of the Lidar data showing the line of the ditch, wall and vallum.....	13

Author

Alex Turner

Research Associate

McCord Centre for Landscape

School of History, Classics and Archaeology

Newcastle University

Newcastle upon Tyne

NE1 7RU

Introduction

As part of the Hadrian's Wall Community Archaeology Project, two sessions of geophysical survey were undertaken in November 2020 and April 2021. The first, an abortive attempt in 2020, was abandoned due to flooding within most of the survey area. The survey failed to produce any useable results. Two successful geophysical surveys were undertaken in April 2021, over a period of two days, in advance of excavation. Due to the restrictions caused by the Covid19 Pandemic, the surveys were undertaken by Alex Turner and Kathryn Murphy of the WallCAP team rather than by volunteers.

Location

The site is located 1100 metres east of Bowness-on-Solway and 700 metres west of Port Carlisle (Figure 1). The site of the milecastle 79, excavated in 1949 and re-evaluated in 1999 (Figure 2), lies 200 metres to the east (Richmond and Gillam 1952, 17 and Willmott 2012, 193). The site is centred on Ordnance Survey grid reference NY 23397 62277 (Figure 1).

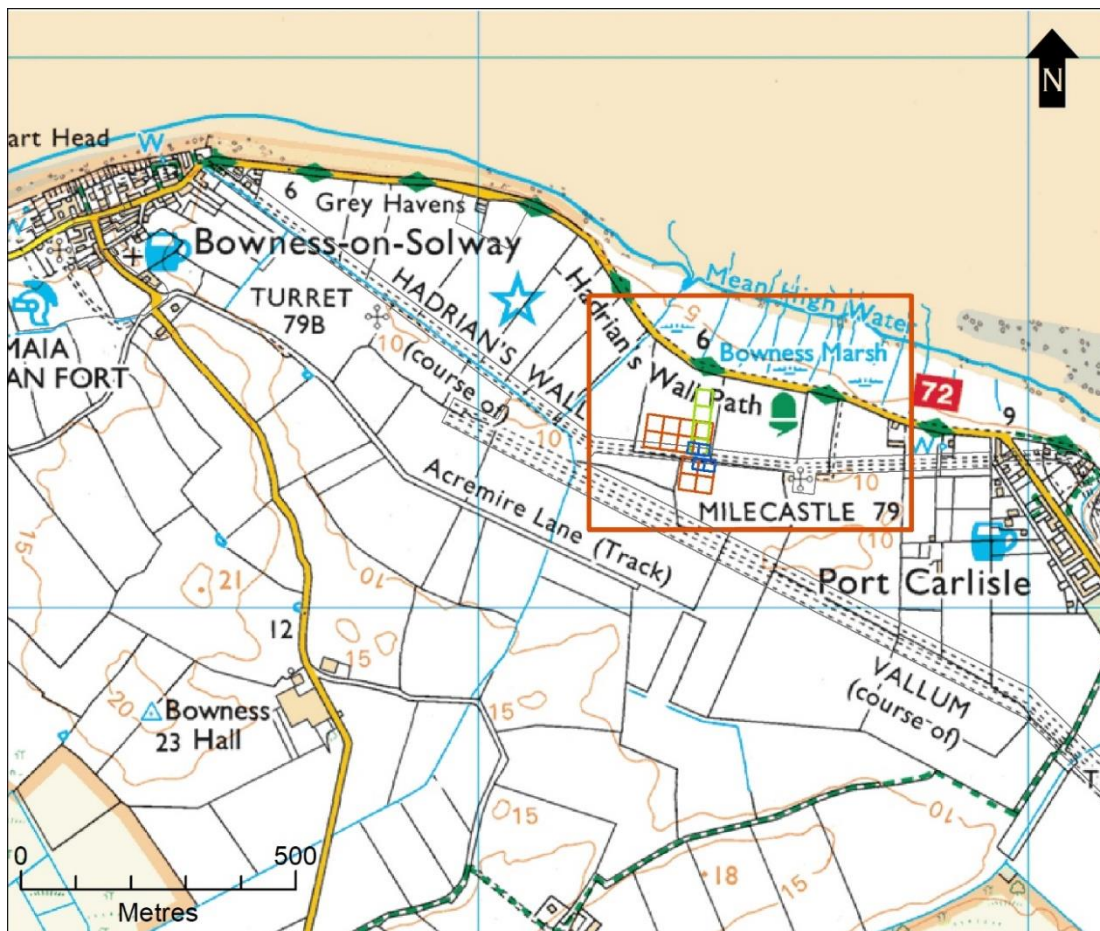


Figure 1 - Location of Port Carlisle. The area of interest is within the red rectangle

The survey area was laid to pasture and divided by a hedge line that ran along the line of the wall to the north and west. A metal gate and fences wire along the field boundary were problematic for gradiometer survey. The area around the gateway showed clear sign of infill, presumably due to the boggy nature of the site in that area. Although the ground was waterlogged and prevented large scale survey in 2020, examination of the flood risk map shows that the site lies south of any major threat of flooding from the saltwater (Figure 3). It was important to establish the line of sea water intrusion in the study area as salt water is a significantly better conductor of electricity than fresh water. This would have implications for any interpretation of the electrical resistance survey. A survey on the interface between the two could potentially lead to highly variable and confusing results. Fortunately, this doesn't seem to have been the case at the Port Carlisle site. An examination of the environment agency sea water flood risk map shows the site to be south of the danger area (Figure 3)



Figure 2 - MC79 excavation 1999 (Wilmott 2012, 193) in relation to geophysics from 2020 and 2021



Figure 3 - Flood risk from the sea in relation to the site location

Topography and Geology

Topography

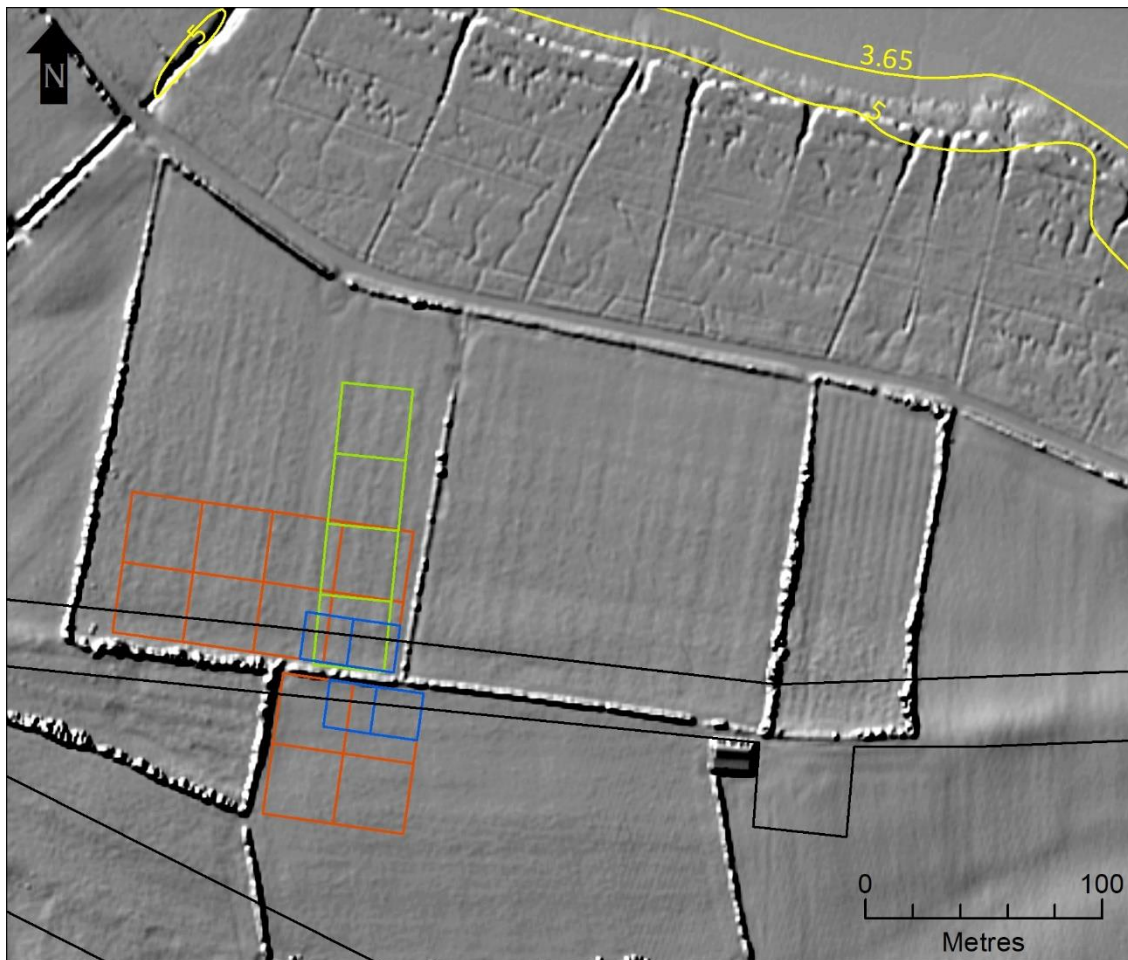


Figure 4 - Lidar digital terrain model (DTM) of the survey areas. The raised line of the wall is clearly visible within the bounds of the World Heritage Site boundary (shown in black).

Examination of the Ordnance Survey contour data and the Environment Agency lidar data (Figure 4) shows a 1.6 metre slope from south to north across the two fields of the survey area. Contours from the five metre Ordnance Survey topographic data show a height of 3.65 metres at the edge of the Solway. This rises to 8 metres where the hedge line, along the top of Hadrian's Wall, divides the two fields. Within the two main survey areas the slope was considerably less with a maximum change in topography, north to south of 0.4 metres. When not waterlogged, this provided ideal condition for consistent gradiometer and resistance surveys.

Geology

The underlying bedrock geology was part of the Mercia mudstone group consisting of mudstone with gypsum-stone and/or anhydrite-stone (Figure 5). These stones are diamagnetic and therefore have no effect on magnetic survey techniques. The superficial geology consisted of a mixture of Gretna Till formation - Diamicton, saltmarsh deposits – clay and silt and intertidal sandflat depots – silt and clay (Figure 6). The soil map showed that the northern half of the survey was categorised as mud and the southern half as sand, clay and gravel (Figure 7). This geological combination, when not waterlogged, enables good survey results to be obtained using either gradiometry or resistivity survey.

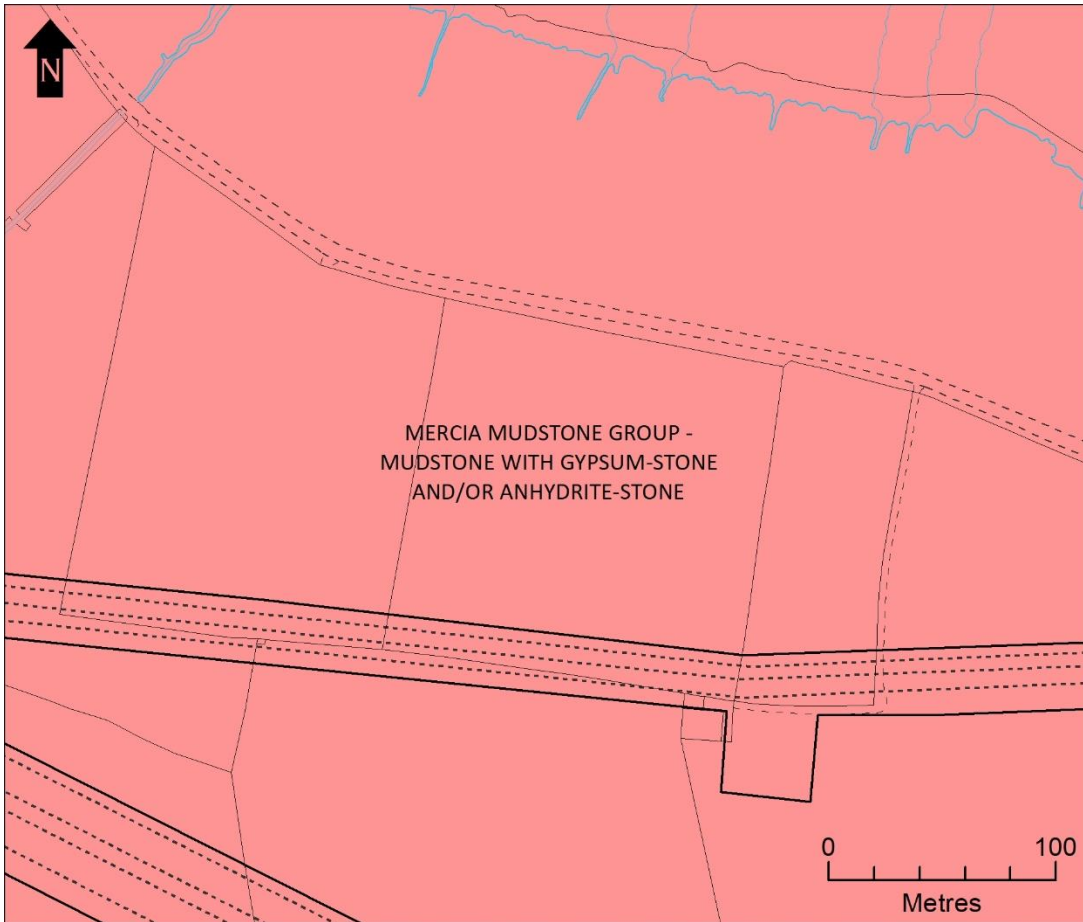


Figure 5 - Bedrock geology for the survey area. BGS 1:50,000 digital geology data.

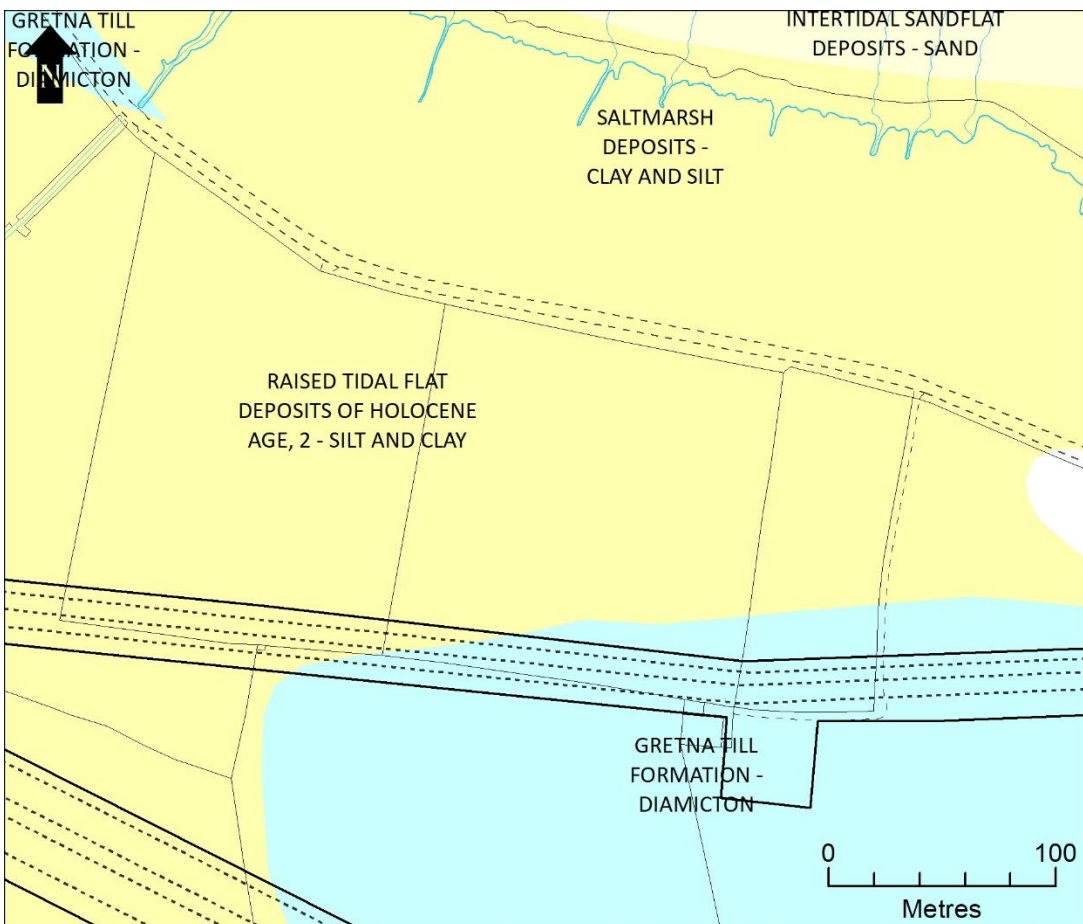


Figure 6 – Superficial geology for the survey area. BGS 1:50,000 digital geology data

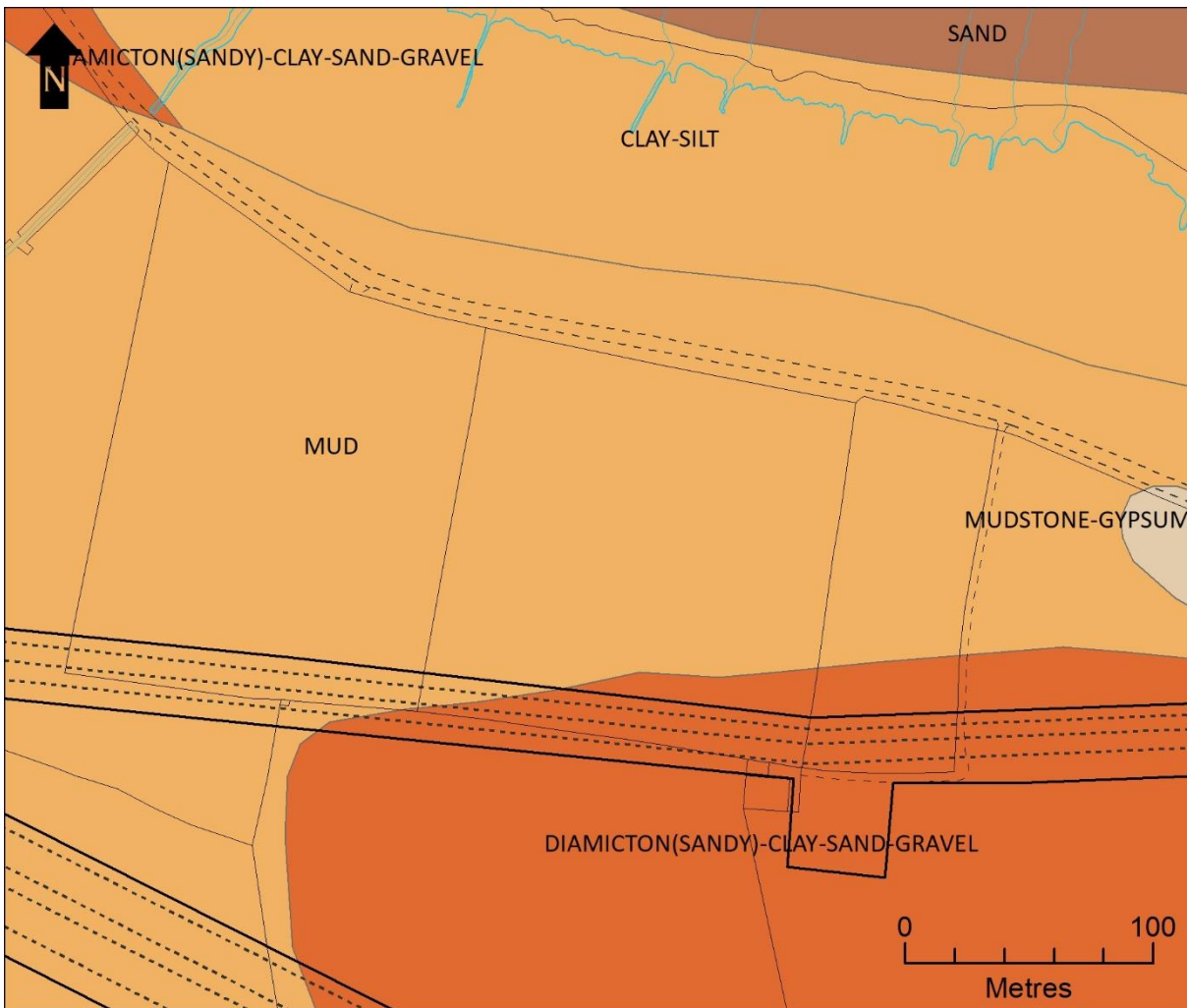


Figure 7 – Soil data (Parent material) for the survey area. BGS 1:50,000 digital geology data

Survey Methodology

Methods - Survey Grids and Markers

For the abortive 2020 survey, four 30m x 30m grid were laid out avoiding large areas of the field that were waterlogged. For the 2021 gradiometer survey, a grid consisting of 12 30m x 30m squares was laid out using a Leica GNSS differential survey grade GPS connected to the Leica RTK Smartnet network. In addition, four 20m x 20m survey grids were laid out for resistivity survey (Figure 8). Temporary grid pegs were used to mark out the grid and the lack of livestock in the fields meant these could be left overnight. The survey grid coordinates were derived from Mastermap digital data and stored as a feature class within the survey ArcGIS geodatabase. Grids were numbered sequentially in a west-east series of rows from north to south. The grid layout was chosen to avoid any close proximity to the ferrous intrusions within the field but in order to survey the area of excavation close proximity to the fence line in the southern field was unavoidable. Fortunately, this area was also covered by a resistivity survey that was unaffected by ferrous intrusions.

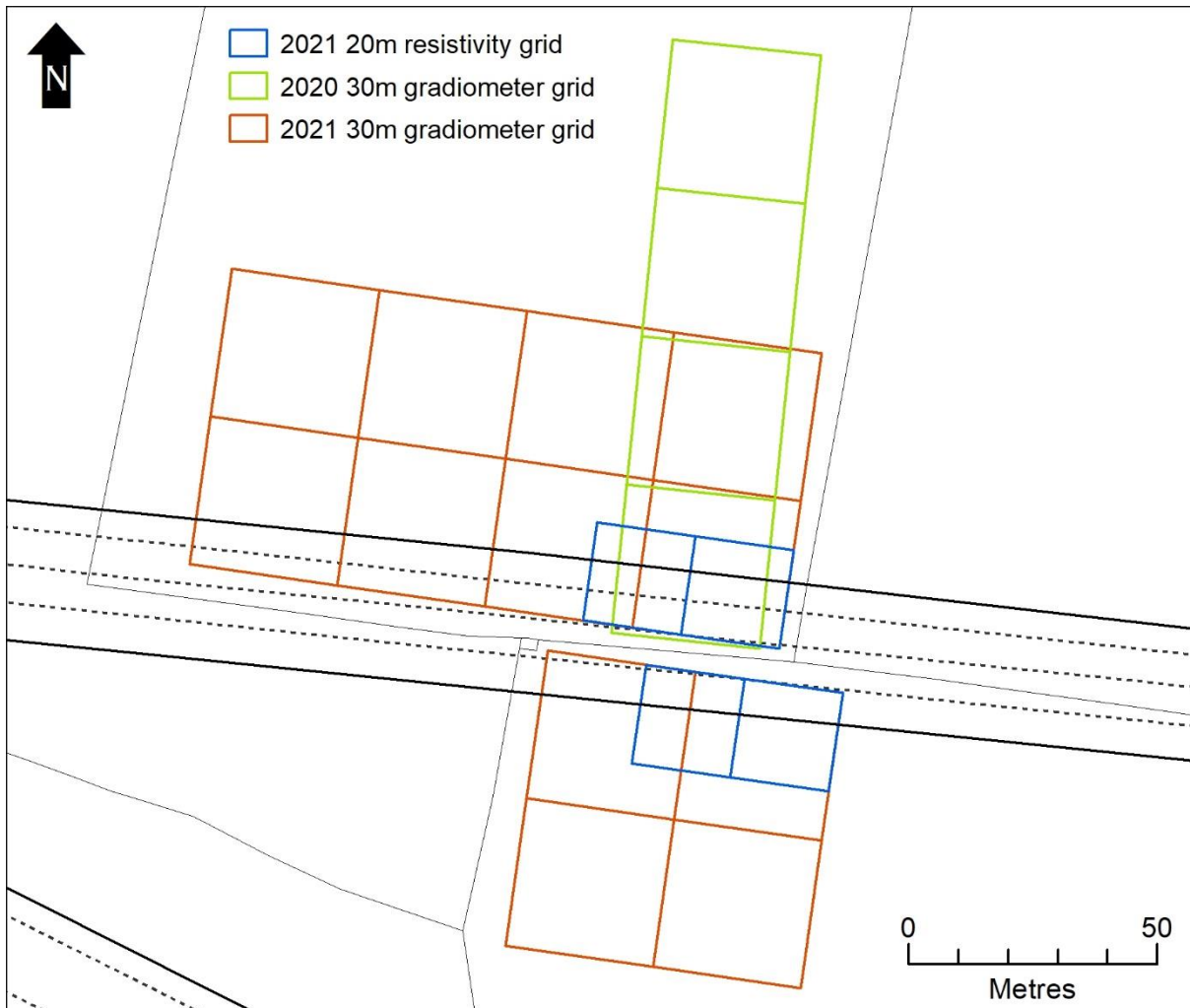


Figure 8 - Location and numbering of the gradiometer survey grids.

Methods - Fluxgate gradiometer survey

The survey was carried out using a Bartington Grad 601/2 fluxgate gradiometer with two vertical sensors spaced one metre apart. Following an initial scan of the survey site, a magnetically sterile area was identified for the creation of the survey control point. This was used to calibrate the gradiometer before each day of survey and after any significant stoppages. In accordance with accepted practice (Schmidt et al 2016, 12) data was collected along a series of zig-zag traverses spaced one meter apart with sample readings being taken every 25 centimetres. This gave an effective resolution of 3600 readings for each 30m x 30m survey grid.

Methods – Electrical resistance survey

Electrical resistance survey was carried out using a Geoscan RM15D Advanced equipped with a MPX15 multiplexer collecting data in parallel twin configuration. The data was collected using a 0.5 metre traverse and 0.5 metre sample to provide a four times greater resolution of survey than a standard 1 metre x 1 metre survey. This gave a resolution for each survey grid of 1600 readings. The enhance survey resolution significantly impacted on survey speed and it was to counterbalance this that a restricted area of four grids in key positions, to the north and south of the proposed excavation, was chosen.

Data processing and presentation

The data from both the resistivity and gradiometer surveys were processed using Geoplot 4.0. The resulting plots were exported as raster images to ArcGIS 7.1 where they were scaled and georeferenced using the latest vectored Mastermap data. This enabled comparison with a combination of modern and historic Ordnance Survey mapping data, Environment Agency Lidar data and aerial photographs downloaded from Digimap. The integration of digital output from the geophysical survey with the Digital Terrain Model (DTM) obtained from the Environment Agency Lidar data also enabled detailed topographic examination of the survey terrain. Digital overlays were created for features identified within the survey output and formed the basis of the final interpretation of the data.

Reference to Historic Ordnance Survey

As part of the interpretation process, an examination of all the editions of the Ordnance Survey at 1:2500, was carried out. Historic Google Earth images were also consulted for the first decade of this century but provided no additional information of significance. The study of the historic maps showed that the arrangement of the survey field boundaries was the same as it is today (Figure 9). It is only to the south of

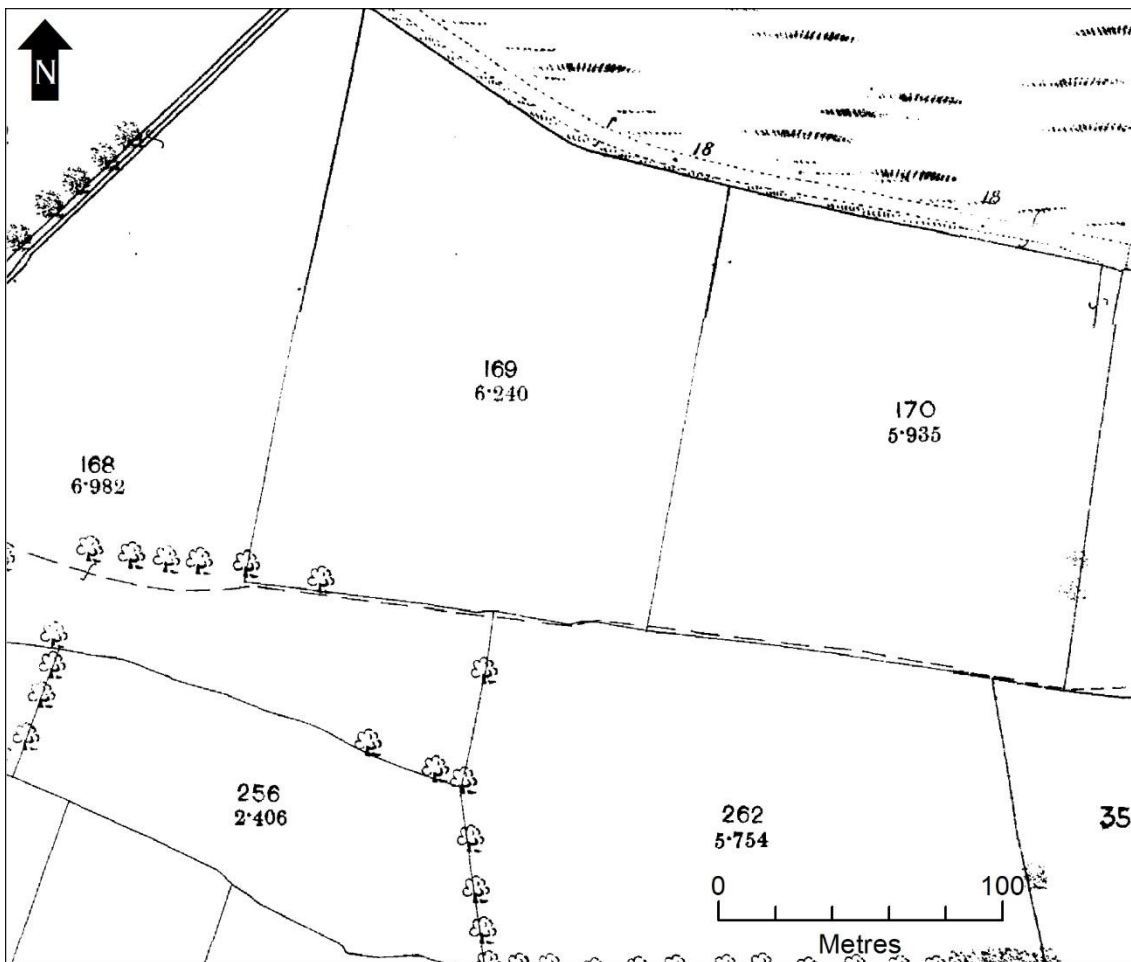


Figure 9 - Field boundary layout shown on the Ordnance Survey 1:2500 County Series 1895

survey area that there is greater sub-division of fields in the nineteenth century. The current gap in the hedge row and the target of the 2021 excavation is shown as a small building straddling the field boundary on the 1:2500 National Grid map for 1970 (Figure). This building doesn't appear on any other Ordnance Survey edition.

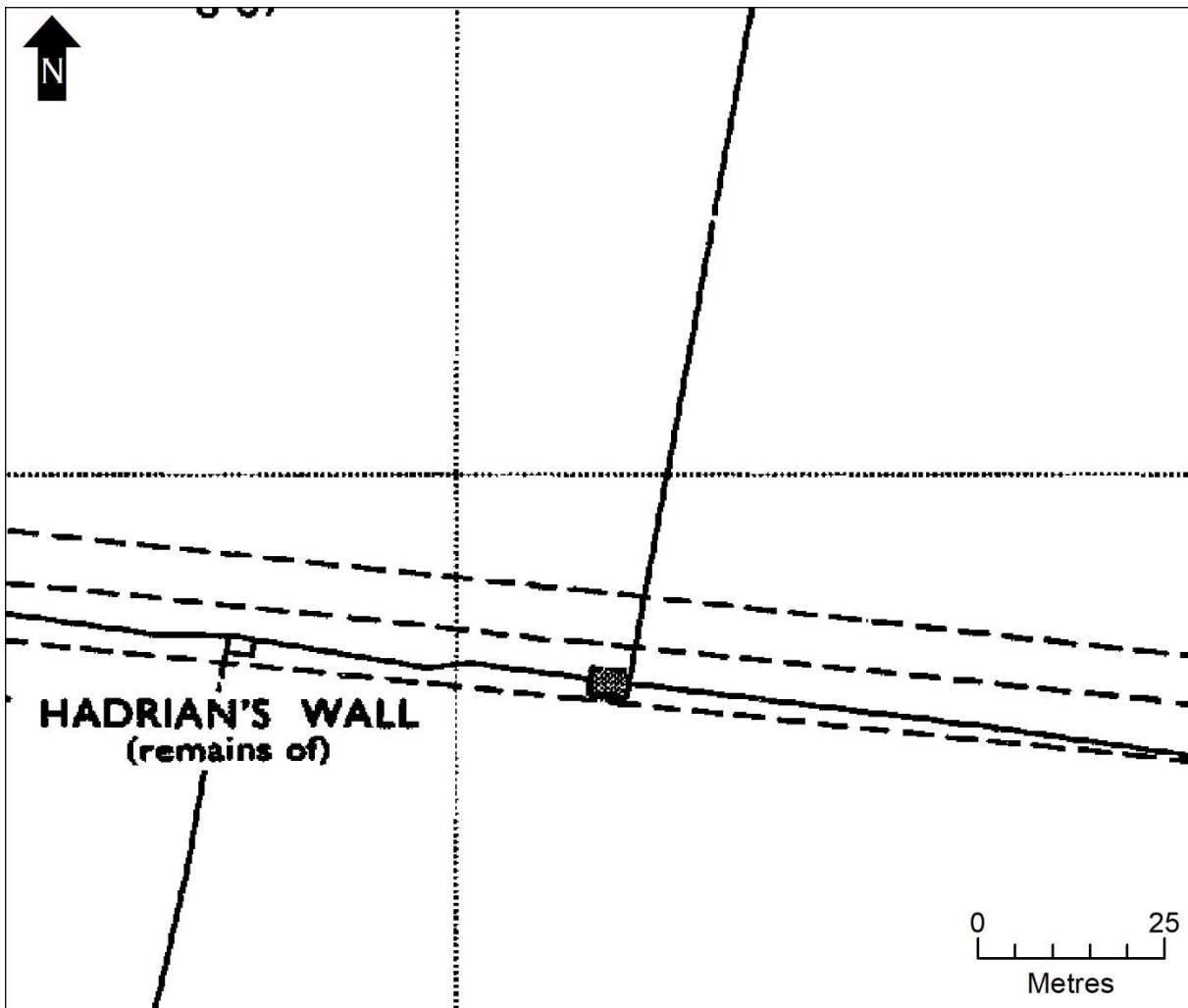


Figure 10 - 1:2500 Ordnance Survey map (1970) showing location of a small building on the field boundary

Survey Results and Interpretation

Gradiometer Results – process summary

The data was processed using Geoplot 4 and exported as a raster image to the ArcGIS 7.1 project for the survey (Figures 11 and 12). Only basic processing was necessary within Geoplot 4. The grids were despiked with a threshold of $\pm 3SD$ and the Zero Mean Traverse filter was applied to reduce any striping as a result of changes in the orientation of the gradiometer during zig-zag survey. A uniform High Pass Filter, to filter any changes in the geological background, was applied with a window of 10 readings in both the X and Y direction. Interpolation was carried out between traverses so that the final data had an X and Y resolution of 0.25 metres. The plots were then scaled and georeferenced to the British National Grid in ArcGIS using coordinates derived from the differential GNSS. The results from the gradiometer survey produced very little of note other than dipolar interference from the metal wire fence.

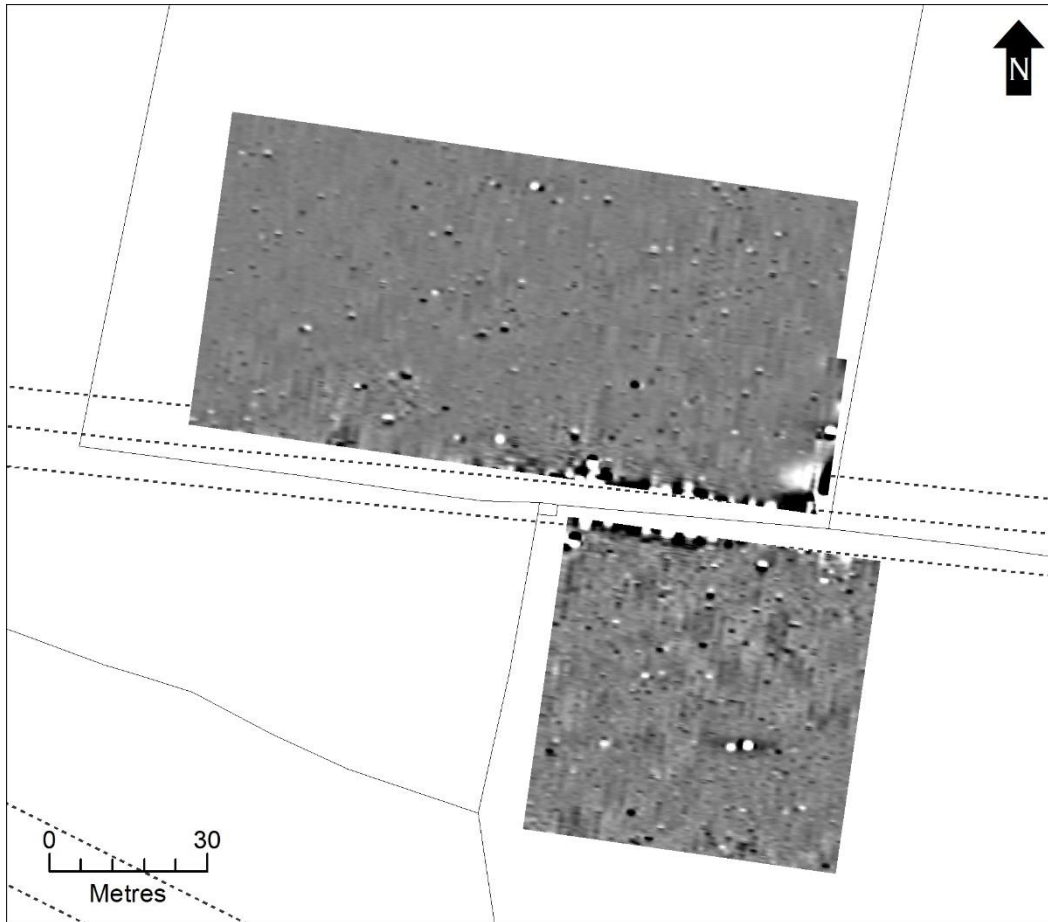


Figure 11 - Plot of the gradiometer survey results

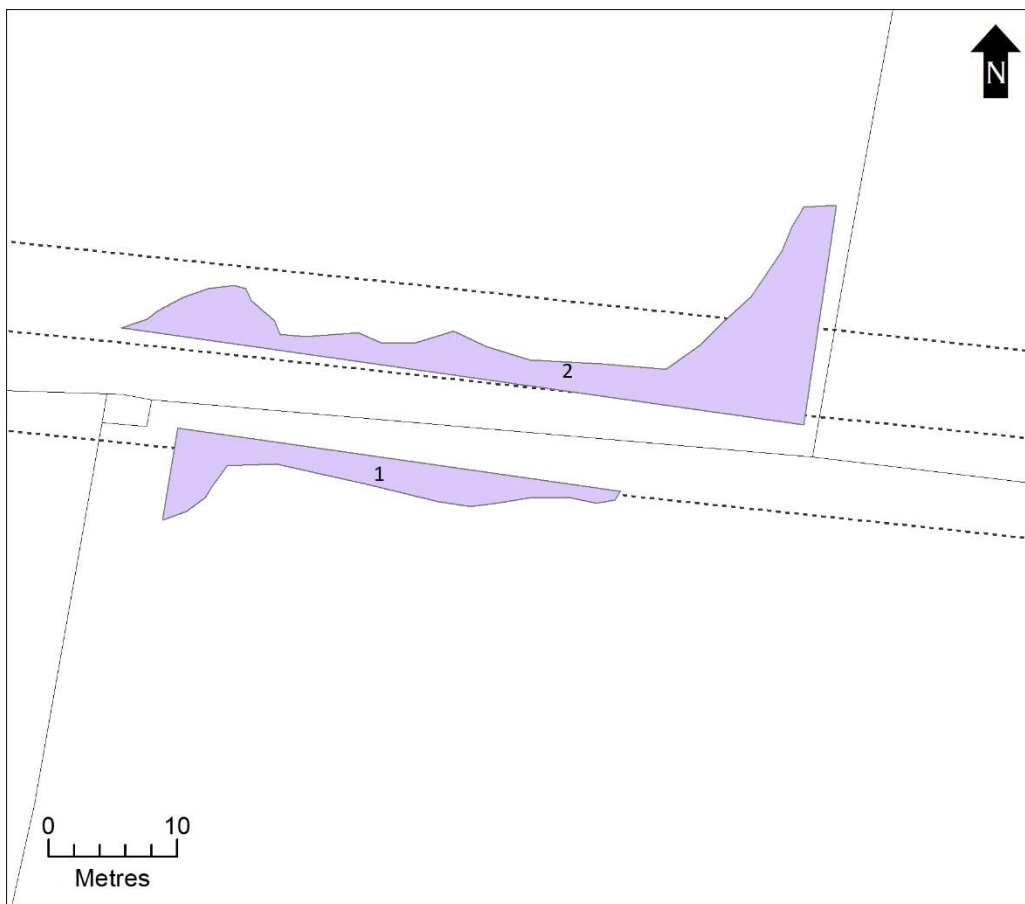


Figure 12 - Interpretation of the gradiometer survey results

Gradiometer Results – Interpretation

The scaled and georeferenced geophysics plots were used to produce an interpretive overlay within ArcGIS. Each of the drawn polygons or polylines was given a unique reference number that is used within the interpretive discussion (Figure 12).

1-2: Dipolar response to metal wire in hedge line.

Resistivity Results – process summary

The data was processed using the same software as the gradiometer survey. The data was despiked with a threshold of +/- 3SD and then a Gaussian high pass filter was applied with a window of 10 readings in the x and y directions to minimise the effect of background geology. A low pass filter with a window of 1 readings in the X and Y directions was used to smooth the data and enhance any large weak features. Interpolation of the data was carried out in the X and Y directions to give data plots with a final spatial resolution of 0.25m x 0.25m. This was an equivalent resolution to the gradiometer data. The results, shown in Figure 12 revealed few archaeological anomalies, consistent with the results from the gradiometer survey.

Resistivity Results – Interpretation

1-5: Ruts from vehicles trapping water to produce a low resistance response.

6: Area of low resistance. Possibly part of wall ditch.

7-8: Areas of high resistance within [6]. Is this wall tumble into ditch?

9-10: Patches of high resistance. Probably associated with areas of disturbance relating to the wall or field bank.

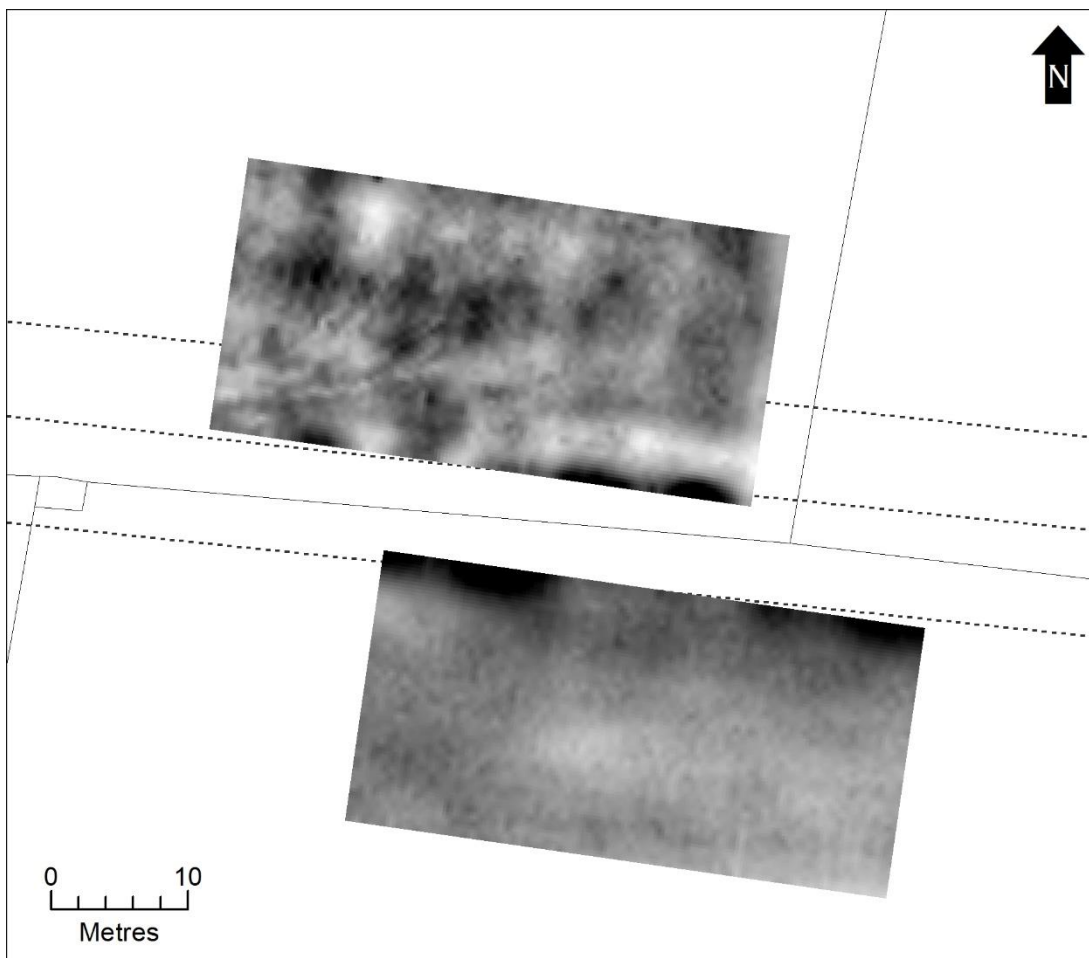


Figure 13 - Plot of results from the resistivity survey

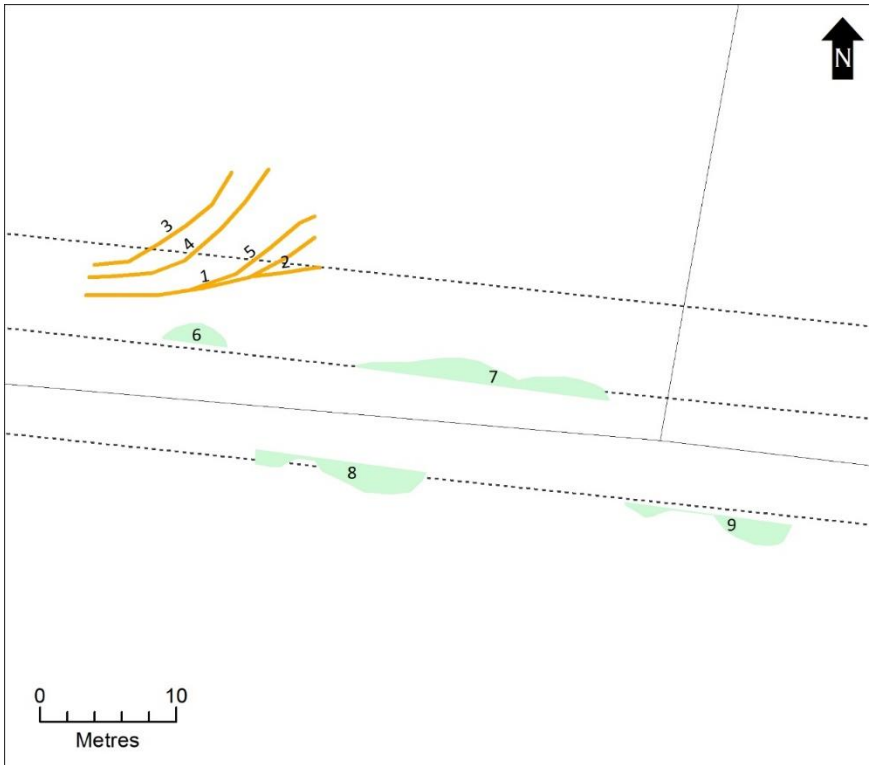


Figure 15 - Interpretation of the resistivity survey results

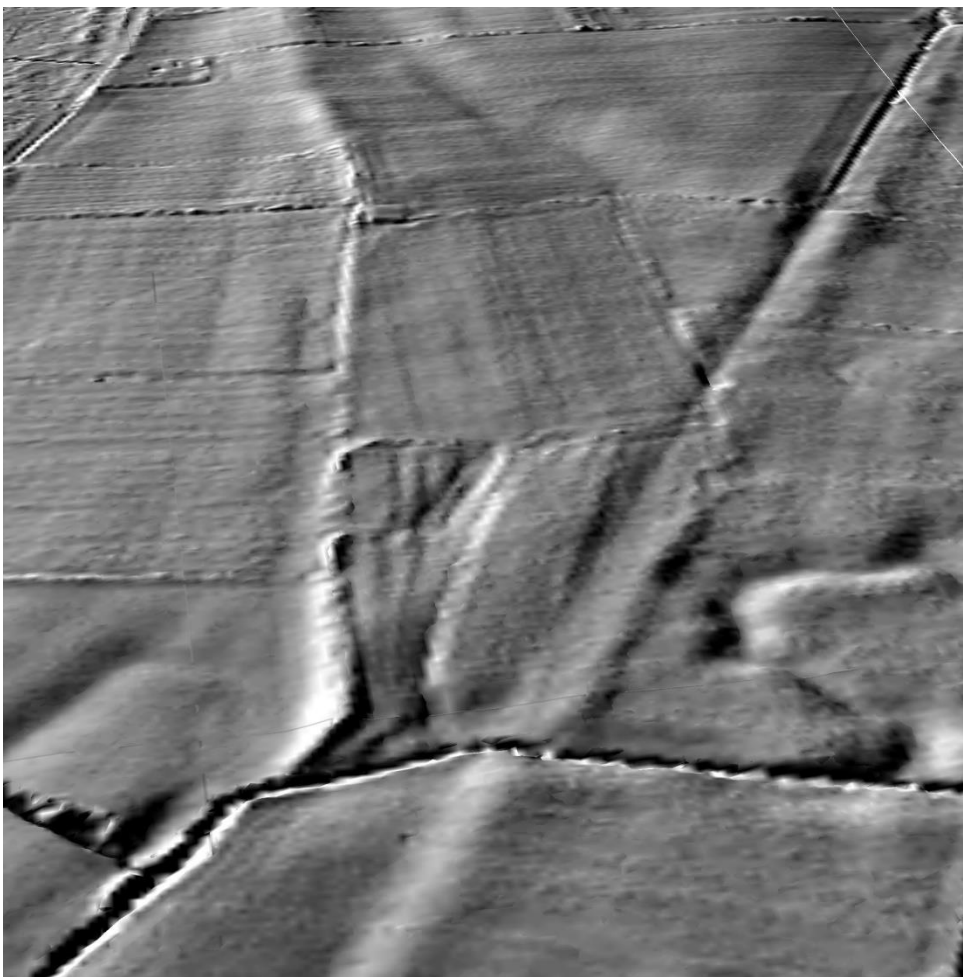


Figure 14 - 3D view of the Lidar data showing the line of the ditch, wall and vallum

Summary

There was limited success with the gradiometer survey with a lack of detection of any sub-surface features. The resistivity survey was successful in detecting some sub-surface features and it is possible that the remains of the wall ditch appear on the plots. The vallum appears as an earthwork on the Lidar and is shown on the 1:2500 Ordnance Survey maps between 1900 and present day but the portion of the vallum located in the fields belonging to the same landowner was 60 metres south of the survey area and therefore not included (Figure 15).

Sources and References

British Geological Survey (2011) - *Soil Parent Material Model [SHAPE geospatial data], Scale 1:50000, updated: 1 June 2011, BGS, using: EDINA Geology Digimap Service, <<https://digimap.edina.ac.uk>>, Downloaded: 2021-05-13 09:35:02.7*

British Geological Survey (2016) *DiGMapGB-50 [SHAPE geospatial data], Scale 1:50000, updated: 30 November 2016, BGS, using: EDINA Geology Digimap Service, <<https://digimap.edina.ac.uk>>, Downloaded: 2021-05-13 09:35:02.7*

Environment Agency (2016) *Lidar Composite Digital Terrain Model England 1m resolution [ASC geospatial data]. Scale 1:4000, Updated: 5 January 2016, Open Government Licence, using: EDINA LIDAR Digimap Service, <<https://digimap.edina.ac.uk>>, Downloaded: 2021-05-13 09:37:04.87*

Ordnance Survey (2021) *1:50,000 Scale Colour Raster [TIFF geospatial data], Scale 1:50,000, updated: 14 May 2021, Ordnance Survey (GB), Using: EDINA Digimap Ordnance Survey Service, <<https://digimap.edina.ac.uk>>, Downloaded: 2021-11-01 09:37:39.084*

Schmidt A, Linford P, Linford N, David A, Gaffney C, Sarris A and Fassbinder J (2016) *EAC Guidelines for the use of Geophysics in Archaeology*

Simpson F, Hodgson K and Richmond I (1934) New Turret-Sites on the Line of the Turf Wall and the Type of Stone Wall Later Associated with Them in *Transactions of the Cumberland and Westmorland Antiquarian and Archaeological Society Series 2 Volume 34*